IDENTIFICATION OF LINES IN THE SPECTRUM OF THE QUASAR 0420 – 388

Y. P. VARSHNI

Department of Physics, University of Ottawa, Canada

(Received 3 October, 1988)

Abstract. The plasma-laser star model for quasars has been used to identify the emission and absorption lines as well as the continuum discontinuity in the spectrum of the quasar 0420 – 388. The He I λ3680 discontinuity is identified for the first time in an astronomical spectra. Two predictions are made.

1. Introduction

In the present paper we identify the emission and absorption lines as well as the continuum discontinuity in the spectrum of the quasar 0420 – 388 on the basis of our theory of quasars (Varshni, 1973, 1974, 1975, 1977a, b, 1978, 1979, 1985, 1988a, b, c; Varshni and Lam, 1976, Varshni and Nasser, 1986). Our theory does not require the superfluous assumption of redshifts and is based on sound physical principles which have been verified in the laboratory.

2. Emission Lines

2.1. The data

There are at least six other quasars which belong to the same spectral class (Varshni, 1976) as 0420 – 388. We summarize the available data on emission lines for all these quasars in Table I. There are a number of other quasars (Hewitt and Burbidge, 1987), which appear to belong to this spectral group but the available data are too poor to make a definite assignment. We give here a partial list of such quasars in two parts:

(a) 0045 – 036, 0114 – 089, 0132 – 197, 0143 – 015, 0143 – 010, 0334 – 204, 1206 + 119, 1251 + 367, 1306 + 294, 1512 + 132, 1607 + 183.

(b) 0116 – 288, 0242 – 301, 0937 + 118, 0938 + 450, 1424 – 118, 1657 + 265.

In the spectra of all of these quasars, the most important feature appears to be a line in the vicinity of 5020 Å. In the redshift hypothesis, some authors have interpreted this line as Lα 1216 Å, resulting in a 'redshift' of about 3.13 for the quasars in the (a) list, while some others have interpeted it as Mg II λ2798 resulting in a 'redshift' of about 0.8 for the quasars in the (b) list. As a matter of fact, one need not stop at 3.13. In the redshift hypothesis, one can argue that the line in question is neither Mg II λ2798, nor Lα λ1216, but He II λ304 (resonance line for this ion), since quasars have been found which do not show Lα λ1216 (Wright *et al.*, 1979; Shaver *et al.*, 1982), and helium is the next most abundant element after hydrogen. Identification of 5020 Å with He II λ304 leads to a 'redshift' of 15.5! After this brief diversion into the fantasy world of the redshift

Astrophysics and Space Science **153**: 153–167, 1989.
© 1989 *Kluwer Academic Publishers. Printed in Belgium.*

© Kluwer Academic Publishers • Provided by the NASA Astrophysics Data System

TABLE I

Emission line data for quasars. For 0537 – 286, set (a), in the second line, below each wavelength, the first figure represents line to continuum ratio, and the second $\Delta\lambda_{1/2}$ (in Å). Similarly, for set (b), the first represents W_λ (in Å), and the second, FWHM (in Å).

Quasar	V (mag)	Set	1 λ (Å)	2 λ (Å)	3 λ (Å)	4 λ (Å)	5 λ (Å)	Source
0420 – 388	16.92		4250	5013	5100	5800		Osmer and Smith (1977)
0140 – 306	18.5			~5020			~6370	Smith *et al.* (1981)
0244 – 3017	19.3			~5000				Wolstencroft *et al.* (1983)
0537 – 286	20	(a)	4238	5000	(5090)	5760	(6302)	Wright *et al.* (1978, 1979)
			0.9, (60)	1.7, (110)	1.0, (70)		(1.0)	
		(b)		5016		5770	6371	Wilkes (1986)
				176		15, 58	163, 258	
1244 + 1129	18.4 (m_J)			~5058				Foltz *et al.* (1987)
1320 – 106	19.5			~5000				Kunth *et al.* (1981)
2228.2 – 4033	19.6	(a)		~5046				Osmer (1979, 1980)
		(b)		~5022				Vaucher *et al.* (1982)

hypothesis, we must get back to reality. We may illustrate the difficulties in assigning a quasar to a spectral class by an example. For the quasar 1251 + 3644, Weedman (1985) reports a single medium strength emission line at 5020 Å. At first sight it would appear to be a good candidate for inclusion in Table I, but the uncertainty in the wavelength is ± 75 Å. It goes to the credit of Weedman that he gives a realistic estimate of the uncertainty. Some comments on the data are given below.

0420 – 388. The wavelengths are from Osmer and Smith (1977) who observed this quasar with a SIT Vidicon Spectrometer on the 1.5 m and 4 m telescopes at CTIO. These authors gives the total equivalent width of line Nos. 2 and 3 to be 132 Å.

0140 – 306. The wavelengths were estimated from the 'redshift' and a low-resolution spectrum given by Smith *et al.* (1981).

0244 – 3017 (= Q1097.1). This quasar was observed by Wolstencroft *et al.* (1983) at low resolution (10.3 Å). The wavelength of the principal emission line was estimated from the spectrum given in Wolstencroft *et al.* (1983). These authors also give the wavelengths of 15 absorption lines.

0537 – 286. Spectroscopic observations of this quasar were made by Wright *et al.* (1978, 1979) at the Anglo-Australian Telescope at low resolution (approximately 10 Å). The values below the wavelengths (first set) in Table I are line-to-continuum ratio and $\Delta\lambda_{1/2}$. Many absorption features were noted in its spectrum and Wright *et al.* (1978) give wavelengths of 22 of these. The second set of data for this quasar in Table I is from Wilkes (1986). In the second line, below each wavelength, the first figure represents W_λ (in Å) and the second, FWHM (in Å).

1244 + 1129. This quasar has been observed by Foltz *et al.* (1987). The wavelength of the principal emission line (Table I) has been estimated from the 'redshift' given by these authors. Absorption lines are visible on the spectrum given by Foltz *et al.* (1987).

© Kluwer Academic Publishers • Provided by the NASA Astrophysics Data System

1320 – 106. Observed by Kunth *et al.* (1981). There is only one strong line in the spectrum whose wavelength in Table I has been estimated from the 'redshift'.

2228.2 – 4033. This quasar has been observed by Osmer (1979, 1980) and by Vaucher *et al.* (1982) but neither gives wavelength(s) of the emission line(s). The two wavelengths listed in Table I have been estimated from the 'redshifts'. Osmer (1979, 1980) notes the presence of absorption lines in the spectrum.

2.2. Line identifications

Line No. 1. No accurate wavelength for this line is available. There are four possible candidates: N II λ4241.8 (mult. 47), N II λ4241.8 (mult. 48), S III λ4253.6 (mult. 4), and C II λ4267 (mult. 6).

Line No. 2. This is the strongest line in these quasars. The best value for the wavelengths appears to be 5013 Å. The spectrum given in Atwood *et al.* (1985) also supports this value. There are two very good candidates for identification of this line: He I λ5015.7 (mult. 4) and C IV $\lambda\lambda$5018, 5017 (mult. 3). Laser action in either of these lines can give rise to the observed line. An emission line at about 5018 Å has been known for many years in Wolf–Rayet spectra. We may note here one point concerning laser action in He I λ5015.7. The lower level for the transition giving rise to this line is metastable. While population inversion, when the lower level is metastable, is not very common, it can occur.

Line No. 3. It appears as a hump on the long wavelength shoulder of line No. 2, and there may be considerable uncertainty in its wavelength. A good candidate for its identification is C II λ5121.7 (mult. 12).

Line No. 4. We identify this line with C IV $\lambda\lambda$5801, 5812 (mult. 1), which is a well-known line in Wolf–Rayet spectra.

Line No. 5. The uncertainty in the wavelength is simply too large to attempt an identification.

3. Absorption-Line Spectrum

We have discussed in previous papers (Varshni, 1977b, 1978, 1985) the characteristics of the absorption-line spectrum of quasars that are predicted from our model. In particular we shall follow the considerations of our 1985 paper.

There has been only one investigation on the absorption-line spectrum of 0420 – 388, that of Atwood *et al.* (1985). Spectra were obtained using the SIT Vidicon detector attached to the echelle spectrograph at the Cassegrain focus of the Cerro Tololo Inter-American Observatory 4 m telescope in October and November 1981. The claimed resolution is 33 km s^{-1} (FWHM). Additional spectra, covering the wavelength range 3815 – 3950 Å were obtained using the Anglo-Australian telescope. When the same quasar has been observed by two or more groups, an intercomparison of the data helps to assess the quality of the data. We have carried out such comparisons for 0805 + 046 (Varshni, 1985) and 0237 – 233 (Varshni, 1988c). Such a comparison is, however, not possible in the present case because only one set of data are available. In

© Kluwer Academic Publishers • Provided by the NASA Astrophysics Data System

a recent paper, Cristiani and Shaver (1988) show, in their Figure 1, an intermediate resolution spectrum of 0420 – 388; however, no wavelengths are listed.

The wavelength discrepancy that one can permit in the identifications depends on the resolution, uncertainty in the wavelength calibration and the width of the line. The claimed resolution in the observations of Atwood *et al.* (1985) is $c/R = 33$ km s^{-1} for most of the wavelength range for which data are reported. This corresponds to $\Delta\lambda = 0.5$ Å at 4500 Å. We do not know how good the wavelength calibration was; we shall assume that any uncertainty due to this reason can be neglected. The real problem lies with the width of the lines. An examination of an enlargement of the spectrum given in Figure 1(a–e) of Atwood *et al.* (1985) shows that many of the lines are wider than 1 Å and appear to be blends (inadequate dispersion?). Some of them are much wider than 1 Å, e.g., line numbers 9, 20, 23, 37, 43, etc. Line No. 174 is approximately 10 Å wide. Taking into account these various factors, a guiding value of 1 Å was taken for the tolerance, i.e., the discrepancy between the observed and identified wavelengths. When the line is very wide (blended) clearly a larger value is acceptable.

We should also note here another problem with the available spectrum. The SIT Vidicon has a more or less conventional silicon diode vidicon preceded by an electrostatic image intensifier stage. It is known that the detective quantum efficiency of silicon diode vidicon is severely reduced at low light levels by amplifier and beam noise (Walker, 1987). Thus the observed spectrum shows only strong single lines and blended medium and weak lines. Many single medium strength and most single weak lines have not been detected. Thus the spectrum is very incomplete. This incompleteness has to be borne in mind while considering the number of lines of any element which are identified as against the expected number of lines, and also as regards the completeness of multiplets in the identifications. We would also like to point out here that Figure 1(a–e) of Atwood *et al.* (1985) shows that there are several lines which are present in the spectrum, but for some reason they have not been recorded in their Table II. In looking for completeness of multiplets we have taken into account such lines; their wavelengths being read from the spectrum. A few of such lines are included in Table II; they do not have a line number.

As regards the relative intensities of lines, for other quasars (Varshni, 1985, 1988c) the available data indicates that the recorded equivalent widths can only be taken as a qualitative guide and this practice was also followed in the present case. Identifications for most of the absorption lines reported by Atwood *et al.* (1985) are presented in Table II. The average value of $|\lambda_{obs} - \lambda_{iden}|$ for all the identifications is 0.69 Å which is quite satisfactory. The representation of some of the elements is as follows.

H. There is an absorption line at 4862.85 Å. Can this line be identified with H_β or not? It is not possible to answer this question with the limited data available. $H\alpha$ is outside the range observed. There is no absorption line at the position of $H\gamma$, but $H\gamma$ could have been weak and easily missed by the detector. There is a line at 4098.05 Å, which is quite near $H\delta$; it is conceivable that $H\delta$, if present, might be a component of this 4098.05 Å line. Clearly better data are required to settle this question. From the available data a low concentration of hydrogen cannot be ruled out. The quasar is

© Kluwer Academic Publishers • Provided by the NASA Astrophysics Data System

certainly deficient in hydrogen, but we do not know to what degree (Kaufmann and Theil, 1980).

He I. Many multiplets are present. The only important line missing is λ5016. Worthy of note is the presence of many lines arising from the 2^1P^0 level.

C II. The presence of the well-known line λ4267 (mult. 6) argues for the presence of this ion.

Mg I. Appears to be present.

Mg II. The well known line λ4481 (mult. 4) is present along with multiplets 9 and 10.

Si I. The strong line λ3906 which arise from the metastable level, $3P^2\ ^1S$, is present, showing the presence of this atom.

Si II. Several lines belonging to multiplets 1, 1.26, 3, 5, and 24 are present.

Ca II. λ 3934 is present.

Ti II. Represented by many lines.

Cr II. Many lines belonging to multiplets 19, 26, 30, 31, and 44 are present.

Fe I. Many lines are present, especially those belonging to multiplets 4, 20, 68, 152, and 318.

Fe II. Well represented by many lines belonging to multiplets 27, 28, 29, 37, 38, etc.

Ni II. Both $\lambda\lambda$3849 and 4067 (mult. 11) are present, as well as two other lines.

Quite a few lines have remained unidentified. There are possible identifications due to ions like Fe III, Y II, Zr II, etc. but because of the incompleteness of the available spectrum, it appears prudent to wait for better observations. Line No. 174 is so wide that we have not tried to propose any identifications. We expect this line to break up into several lines under better dispersion and resolution.

The other six quasars in Table I also show absorption lines. 0420 – 388 is, of course, the brightest. It is obvious that high dispersion, high resolution studies of the absorption line spectrum of this quasar (and of the other six) with instrumentation capable of detecting weak lines would be most worthwhile.

4. The Discontinuity near 3700 Å

Before coming to a discussion and identification of a discontinuity near 3700 Å in the continuum of the quasars listed in Table I, first we give a brief summary of the essential features of a discontinuity in stellar continuum.

A remarkable feature in stellar spectra are the jumps near the limits of the different series. This is a consequence of the discontinuous variation of the absorption coefficient. On crossing a series limit from higher to lower wavelengths, the absorption coefficient increases discontinuously. Consequently the outgoing radiation flux decreases discontinuously at these wavelengths. The most commonly observed discontinuity in stellar spectra is of course the Balmer discontinuity at 3646 Å.

Figure 1 is a schematic representation of the behaviour of the continuum near a discontinuity. The magnitude of the discontinuity is usually defined by Chalonge and Divan (1952) or Aller (1963) as

$$D = \log_{10}(I_+/I_-)\,,$$

© Kluwer Academic Publishers • Provided by the NASA Astrophysics Data System

TABLE II

Identification of lines in the spectrum of 0420 − 388.
$\delta = \lambda_{obs} - \lambda_{lab}$. λ_{obs}, W_λ, λ_{lab}, and δ all are in Å.

n	λ_{obs}	W_λ	Identification			δ
			λ_{lab}	Ion	Mult.	
1	3819.38	1.65	3819.61	He I	22	−0.23
			3820.43	Fe I	20	−1.05
	3824.50		3824.44	Fe I	4	0.06
			3824.91	Fe II	29	−0.41
			3825.88	Fe I	20	−1.38
2	3830.21	8.50	3829.35	Mg I	3	0.85
	3833.50		3832.30	Mg I	3	1.20
			3834.22	Fe I	20	−0.73
3	3841.47	1.76	3840.44	Fe I	20	1.03
			3841.05	Fe I	45	0.42
4	3849.15	1.63	3849.58	Ni II	11	−0.43
			3849.97	Fe I	20	−0.82
5	3854.15	1.15	3853.66	Si II	1	0.49
6	3858.62	0.78	3858.35	v Sag		
			3859.91	Fe I	4	−1.29
	3862.00		3862.59	Si II	1	−0.59
7	3869.29	1.72	3869.56	Fe I		−0.27
8	3872.91	2.12	3871.82	He I	60	1.09
			3872.50	Fe I	20	0.41
			3872.76	Fe II	29	0.15
9	3881.22	7.56	3878.18	He I	59	3.04
			3881.92	Ni II	13	−0.70
			3882.28	Ti II	34	−1.06
	3884.50		3884.85	V II	33	−0.35
10	3888.67	0.83	3888.65	He I	2	0.02
11	3893.17	0.64	3892.30	Cr II		0.87
12	3900.66	2.61	3899.71	Fe I	4	0.95
			3900.55	Ti II	34	0.11
			3900.68	Al II	1	−0.02
13	3906.79	1.28	3905.53	Si I	3	1.26
			3905.64	Cr II	167	1.15
			3906.04	Fe II	173	0.75
			3906.48	Fe I	4	0.31
14	3910.20	2.99	3909.64	v Sag		
			3911.14	ε Aurigae		
15	3920.07	2.60	3920.26	Fe I	4	−0.19
	3926.50		3926.53	He I	58	−0.03
	3928.50		3927.92	Fe I	4	0.58
16	3934.70	1.58	3933.66	Ca II	1	1.04
			3935.91	He I	57	−1.21
17	3945.81	3.90	3945.11	Cr II		0.70
			3945.21	Fe II	3	0.60
18	3951.23	2.14	3951.97	V II	10	−0.74
19	3963.89	3.50	3964.57	Fe II	29	−0.68
			3964.73	He I	5	−0.84

© Kluwer Academic Publishers • Provided by the NASA Astrophysics Data System

Table II (continued)

n	λ_{obs}	W_λ	Identification			δ
			λ_{lab}	Ion	Mult.	
20	3973.86	6.26	3973.64	V II	9	0.22
			3974.16	Fe II	29	– 0.30
			3975.03	Fe II	191	– 1.17
21	3981.99	1.98	3981.62	Fe II	3	0.37
			3982.00	Ti II	11	– 0.01
	3987.00		3987.63	Ti II	11	– 0.63
22	3992.00	4.92	3991.14	Zr II	30	0.86
			3992.06	α Cygni		
23	3999.69	5.81	3998.98	Zr II	16	0.71
24	4004.61	1.78	4005.25	Fe I	43	– 0.64
			4005.71	V II	32	– 1.10
	4010.50		4009.26	He I	55	1.24
	4025.50		4024.55	Fe II	127	0.95
			4026.19	He I	18	– 0.69
			4026.36	He I	18	– 0.86
25	4031.05	1.71	4029.68	Zr II	41	1.37
			4031.46	Fe II	151	– 0.41
26	4037.30	2.10	4036.78	V II	9	0.52
			4038.03	Cr II	194	– 0.73
27	4043.63	2.34	4044.01	Fe II	172	– 0.38
28	4051.76	2.96	4051.21	Fe II	172	0.55
			4051.34	V II	215	0.42
			4051.97	Cr II	19	– 0.21
29	4067.07	1.71	4067.05	Ni II	11	0.02
30	4077.34	1.46	4077.71	Sr II	1	– 0.37
31	4082.00	2.39	4082.30	Cr II	165	– 0.30
32	4090.39	2.52	4088.90	Cr II	19	1.49
			4090.52	Zr II	29	– 0.13
33	4098.05	1.14	4098.44	Cr II	165	– 0.39
34	4119.70	4.20	4118.55	Fe I	801	1.15
			4119.53	Fe II	21	0.17
			4120.81	He I	16	– 1.11
			4120.99	He I	16	– 1.29
	4122.50		4122.64	Fe II	28	– 0.14
35	4128.73	1.20	4128.05	Si II	3	0.68
			4128.73	Fe II	27	– 0.01
36	4133.68	0.97	4132.41	Cr II	26	1.27
			4132.90	Fe I	357	0.78
			4134.68	Fe I	357	– 1.00
	4138.50		4138.40	Fe II	39	0.10
37	4145.93	7.94	4143.76	He I	53	2.17
			4145.77	Cr II	162	0.16
			4147.26	Fe II	141	– 1.33
38	4153.23	1.17	4152.98	Fe II	45	0.25
			4153.91	Fe I	695	– 0.68
39	4155.69	1.61	4154.81	Fe I	694	0.88
			4156.24	Zr II	29	– 0.55
			4156.80	Fe I	354	– 1.11

© Kluwer Academic Publishers • Provided by the NASA Astrophysics Data System

Table II (continued)

n	λ_{obs}	W_λ	Identification			δ
			λ_{lab}	Ion	Mult.	
40	4161.12	1.89	4160.62	Fe II	39	0.50
			4161.52	Ti II	21	−0.40
	4178.00		4177.70	Fe II	21	0.30
			4178.85	Fe II	28	−0.85
41	4180.43	0.82	4179.43	Cr II	26	1.00
			4181.76	Fe I	354	−1.33
	4184.50		4183.20	Fe II	21	1.30
			4183.43	V II	37	1.06
			4184.33	Ti II	21	0.17
42	4187.27	0.84	4187.04	Fe I	152	0.23
			4187.80	Fe I	152	−0.53
43	4191.15	5.98	4190.29	Ti II	21	0.86
			4190.74	Si II	1.26	0.41
			4192.07	Ni II	10	−0.92
44	4203.26	1.29	4202.03	Fe I	42	1.23
			4202.35	V II	25	0.91
45	4208.23	1.09	4207.35	Cr II	26	0.88
			4208.99	Zr II	41	−0.76
46	4217.17	1.51	4215.52	Sr II	1	1.65
			4217.55	Fe I	693	−0.38
47	4225.09	2.47	4224.85	Cr II	162	0.24
			4225.46	Fe I	693	−0.37
48	4233.39	1.56	4233.17	Fe II	27	0.22
			4233.61	Fe I	152	−0.22
49	4235.26	1.45	4235.94	Fe I	152	−0.68
50	4240.93	1.70	4240.49	v Sag		
			4242.38	Cr II	31	−1.45
	4247.50		4246.83	Sc II	7	0.67
51	4253.11	0.69	4252.62	Cr II	31	0.49
			4254.35	Cr I	1	−1.24
	4259.50		4258.15	Fe II	28	1.35
52	4266.38	0.46	4266.97	Fe I	273	−0.59
			4267.02	C II	6	−0.64
53	4270.12	1.06	4269.28	Cr II	31	0.84
			4271.16	Fe I	152	−1.04
54	4278.92	2.04	4278.13	Fe II	32	0.79
			4278.89	V II	225	0.03
55	4281.03	1.88	4280.55	HD 30353		
			4282.41	Fe I	73	−1.38
56	4285.64	2.43	4284.21	Cr II	31	1.43
			4286.28	Fe II	222	−0.64
57	4288.80	1.32	4287.89	Ti II	20	0.91
			4290.22	Ti II	41	−1.42
58	4292.96	1.08	4294.10	Ti II	20	−1.14
59	4298.14	3.58	4299.24	Fe I	152	−1.10
60	4314.03	1.43	4312.86	Ti II	41	1.17
			4314.08	Sc II	15	−0.05
			4314.29	Fe II	32	−0.26
			4314.98	Ti II	41	−0.95

© Kluwer Academic Publishers • Provided by the NASA Astrophysics Data System

Table II (continued)

n	λ_{obs}	W_λ	Identification			δ
			λ_{lab}	Ion	Mult.	
61	4316.96	1.81	4316.81	Ti II	94	0.15
62	4318.96	0.83	4318.22	Fe II	220	0.74
			4319.72	Fe II	220	−0.76
63	4321.13	0.79	4320.74	Sc II	15	0.39
			4320.97	Ti II	41	0.16
64	4367.99	0.61	4367.66	Ti II	104	0.33
			4368.26	Fe II		−0.27
			4369.40	Fe II	28	−1.41
65	4372.21	1.77	4372.22	Fe II	33	−0.01
66	4391.03	1.58	4390.58	Mg II	10	0.44
			4390.98	Ti II	61	0.05
67	4395.63	1.62	4395.03	Ti II	19	0.60
			4395.85	Ti II	61	−0.22
68	4398.16	0.60	4398.31	Ti II	61	−0.15
69	4405.49	0.48	4404.75	Fe I	41	0.74
70	4408.99	0.38	4409.22	Ti II	61	−0.23
71	4416.71	0.68	4416.82	Fe II	27	−0.11
			4417.72	Ti II	40	−1.01
72	4433.28	0.64	4433.99	Mg II	9	−0.71
73	4438.81	2.84	4437.55	He I	50	1.26
			4438.01	α Cygni		
74	4444.50	3.05	4443.80	Ti II	19	0.70
			4444.56	Fe II	201	−0.06
			4444.56	Ti II	31	−0.06
75	4447.46	1.04	4446.25	Fe II	187	1.21
			4447.72	Fe I	68	−0.26
76	4450.33	2.86	4449.66	Fe II	222	0.67
			4450.49	Ti II	19	−0.16
			4451.54	Fe II		−1.22
77	4455.34	0.49	4455.26	Fe II		0.08
78	4456.75	0.39	4456.65	Ti II	115	0.10
79	4458.53	1.14	4458.02	v Sag		
			4459.12	Fe I	68	−0.59
80	4465.57	2.52	4464.47	Ti II	40	1.10
			4466.55	Fe I	350	−0.98
81	4471.13	1.25	4470.86	Ti II	40	0.27
			4471.48	He I	14	−0.35
			4471.69	He I	14	−0.56
82	4480.30	1.77	4481.13	Mg II	4	−0.83
			4481.33	Mg II	4	−1.03
83	4482.19	1.25	4482.26	Fe I	68	−0.07
84	4488.10	2.62	4488.32	Ti II	115	−0.22
			4489.18	Fe II	37	−1.08
85	4491.58	2.40	4491.30	Fe II	37	0.28
86	4496.28	0.95	4495.46	Fe II		0.82
87	4499.69	1.26				
88	4503.34	1.40	4504.52	Cr II	16	−1.18
89	4506.01	0.45	4507.19	Cr II		−1.18
			4507.20	Fe II	213	−1.19

© Kluwer Academic Publishers • Provided by the NASA Astrophysics Data System

Table II (continued)

n	λ_{obs}	W_λ	Identification			δ
			λ_{lab}	Ion	Mult.	
90	4516.65	0.61	4515.34	Fe II	37	1.31
91	4520.64	0.47	4520.22	Fe II	37	0.41
92	4522.65	2.07	4522.63	Fe II	38	0.02
93	4524.47	0.66	4524.73	Ti II	60	−0.26
94	4525.91	0.97	4526.58	Fe II	171	−0.67
95	4532.59	2.70	4533.97	Ti II	50	−1.38
96	4536.70	1.50	4535.84	*v* Sag		
97	4541.74	1.27	4541.52	Fe II	38	0.22
98	4544.94	0.49	4545.74	Ti II	30	−0.80
99	4553.25	1.57	4552.30	Ti II	30	0.95
			4552.65	Si III	2	0.60
100	4558.52	1.37	4558.66	Cr II	44	−0.14
101	4562.01	1.78	4563.35	Ti II	50	−1.34
102	4565.11	0.89	4563.76	Ti II	50	1.35
			4564.55	V II	56	0.56
			4565.58	Cr II	39	−0.47
103	4569.57	1.03	4568.31	Ti II	60	1.26
104	4574.33	0.43	4574.78	Si III	2	−0.45
105	4585.03	0.64	4583.83	Fe II	38	1.20
106	4589.22	1.54	4588.22	Cr II	44	1.00
			4589.96	Ti II	50	−0.74
107	4596.52	1.89	4595.68	Fe II	38	0.84
108	4598.73	1.44	4598.53	Fe II	219	0.20
			4600.19	V II	56	−1.46
109	4603.33	3.28				
110	4620.59	0.61	4620.51	Fe II	38	0.08
111	4625.70	0.85	4625.55	Fe II	219	0.15
			4625.91	Fe II	186	−0.21
112	4628.33	1.45	4629.34	Fe II	37	−1.01
113	4630.60	1.81	4630.54	N II	5	0.06
			4631.89	Fe II	219	−1.29
114	4635.28	3.84	4634.11	Cr II	44	1.17
			4635.33	Fe II	186	−0.05
115	4645.28	2.17	4644.05	Fe II		1.23
116	4647.37	2.00	4648.17	Fe II		−0.80
117	4649.50	0.89	4648.93	Fe II	25	0.57
118	4651.00	0.46	4652.28	Fe II	219	−1.28
119	4663.85	2.45	4663.10	Ti II	38	0.75
			4663.70	Fe II	44	0.15
	4669.50		4670.17	Fe II	25	−0.67
120	4671.43	1.21	4670.40	Sc II	24	1.03
121	4678.36	1.93	4678.85	Fe I	821	−0.49
122	4681.57	0.45	4681.10	S II		0.47
123	4693.52	2.39	4693.23	*v* Sag		
124	4701.17	0.87	4700.26	S II		0.91
125	4705.34	0.57				
126	4713.12	0.52	4713.14	He I	12	−0.02
			4713.37	He I	12	−0.25

© Kluwer Academic Publishers • Provided by the NASA Astrophysics Data System

Table II (continued)

n	λ_{obs}	W_λ	Identification			δ
			λ_{lab}	Ion	Mult.	
127	4715.50	1.40	4716.32	Si III		– 0.82
	4721.00		4719.51	Ti II	59	1.48
128	4725.19	2.73				
129	4730.45	0.44	4730.36	Mn II	5	0.09
			4731.44	Fe II	43	– 0.99
130	4744.30	0.78				
131	4747.71	0.73				
132	4752.37	1.15	4751.82	Na I	11	0.55
133	4758.57	1.11				
134	4760.36	1.37	4761.38	Cr II		– 1.02
135	4777.29	1.29	4775.91	C I	6	1.38
136	4783.14	3.58	4784.64	v Sag		
137	4790.47	2.18	4791.31	v Sag		
138	4793.07	1.34	4792.39	Ti II	48	0.68
139	4796.87	0.52	4796.34	v Sag		
140	4802.73	4.39	4801.80	O I	15	0.93
			4803.27	N II	20	– 0.54
141	4807.67	0.55	4806.67	HD 30353		
142	4814.90	1.88	4814.76	v Sag		
143	4817.70	0.69	4817.33	C I	5	0.20
144	4820.54	2.20	4820.95	Ti II		– 0.41
145	4824.21	0.56	4824.13	Cr II	30	0.08
146	4832.51	0.64	4833.21	Fe II	30	– 0.70
147	4836.79	3.18	4836.22	Cr II	30	0.57
148	4844.16	0.85	4844.98	v Sag		
149	4846.61	1.49	4846.50	Fe II		0.11
150	4849.69	0.76	4848.24	Cr II	30	1.45
151	4857.63	1.35	4856.19	Cr II	30	1.44
152	4862.85	1.39				
153	4865.36	0.45	4864.32	Cr II	30	1.04
			4865.62	Ti II	29	– 0.26
154	4870.24	0.81	4871.32	Fe I	318	– 1.08
155	4874.70	1.52	4874.02	Ti II	114	0.68
156	4876.00	0.93	4876.41	Cr II	30	– 0.41
157	4877.06	1.11				
158	4880.58	0.36	4880.80	HD 30353		
159	4882.89	1.20	4883.20	Si II	24	– 0.31
			4883.41	V II	209	– 0.52
160	4885.96	2.90	4884.57	Cr II	30	1.39
161	4888.75	1.37				
162	4898.08	0.71				
163	4899.95	2.48				
164	4904.41	0.62	4903.32	Fe I	318	1.09
165	4906.09	1.14	4906.88	Si II		– 0.79
166	4909.91	0.37	4911.20	Ti II	114	– 1.30
167	4917.33	0.94	4917.40	HD 30353		
168	4918.86	1.02	4919.00	Fe I	318	– 0.14
169	4920.56	0.70	4921.93	He I	48	– 1.37
			4920.51	Fe I	318	0.05

© Kluwer Academic Publishers • Provided by the NASA Astrophysics Data System

Table II (continued)

n	λ_{obs}	W_λ	Identification			δ
			λ_{lab}	Ion	Mult.	
170	4928.72	2.54				
171	4932.06	2.57	4932.00	C I	13	0.06
172	4940.99	0.90				
173	4951.55	1.24	4951.65	Fe II		−0.10
			4952.78	Cr II		−1.23
174	4966.10	20.0				
175	4983.15	1.12	4982.51	Fe I	1067	0.64
			4983.86	Fe I	1066	−0.71
176	4992.00	1.87	4991.11	Fe II	25	0.89
177	4993.86	0.65	4993.36	Fe II	36	0.50
178	5000.94	0.58	5001.70	α Cygni		
179	5024.28	0.92	5022.87	Fe II		1.41
180	5033.07	0.88	5032.79	Fe II		0.28
181	5048.17	1.58	5047.69	Fe II		0.48
			5047.74	He I	47	0.43
182	5057.01	0.71	5056.35	Si II	5	0.66
183	5093.19	0.77	5093.47	Fe II	205	−0.28
184	5101.86	0.39	5100.84	Fe II	185	1.02
185	5148.77	1.71	5149.54	Fe II		−0.77
186	5151.44	0.82	5150.93	Fe II		0.51

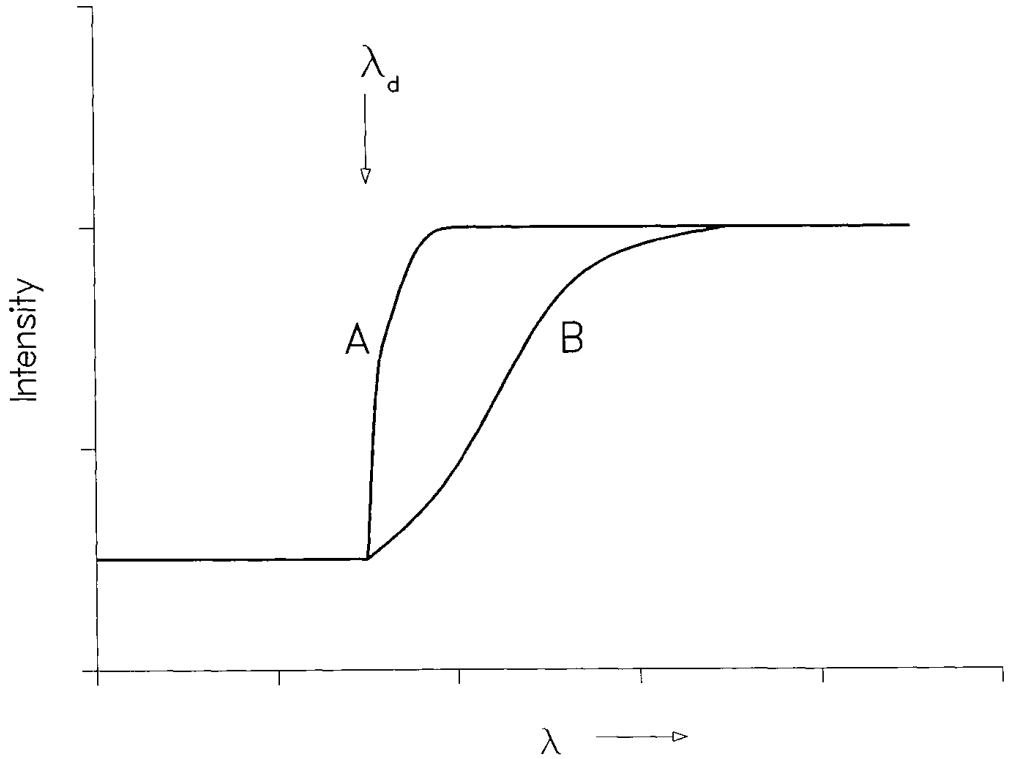

Fig. 1. Shape of a discontinuity in stellar continuum spectral energy distribution. The drop can be rather sharp (curve *A*) or it can be very smooth and gentle (curve *B*).

© Kluwer Academic Publishers • Provided by the NASA Astrophysics Data System

where I_+ and I_- are the intensities for the long- and short-wavelength sides of the discontinuity (λ_d). The quantity D depends on stellar conditions, i.e., T_e, P_e and the composition. The shape of the continuum for $\lambda > \lambda_d$ for two extreme cases is shown in Figure 1. The drop can be rather sharp (curve *A*) or it can be very smooth and gentle (curve *B*). And, of course, various intermediate cases are possible and are found to occur. In the neigbourhood of λ_d on the long wavelength side, if the depression of the continuum is substantial, the coalescence of the higher lines of the series may shift the apparent discontinuity to longer wavelengths. This effect is more pronounced at low resolution.

Next we summarize the evidence on the discontinuity in the continuum of quasars listed in Table I.

0420 – 388. The spectrum given in Smith *et al.* (1981) indicates the position of the discontinuity to be at about 3760 Å but the spectrum is very noisy in this region.

0140 – 306. Smith *et al.* (1981) give the position of the discontinuity as 3665 Å.

0244 – 3017. Wolstencroft *et al.* (1983) state that a sharp drop in the continuum occurs near 3740 Å.

0537 – 286. Wright *et al.* (1978) observed an extremely sharp drop in the continuum level shortward of 3650 Å. Wilkes (1986) finds the discontinuity to occurs at 3633 Å. However, the noise level of the spectrum (Wilkes *et al.*, 1983) shortward of the discontinuity indicates that the discontinuity could equally well be at a longer wavelength by as much as 50 Å.

1244 + 1129. From the spectrum given in Foltz *et al.* (1987), we estimate the position of the discontinuity to be at about 3720 Å.

1320 – 106. Kunth *et al.* (1981) give the spectrum of this quasar, but it is very noisy, especially in the region of the discontinuity. From their Figure 2(d) (POX 175), we estimate 3700 ± 30 Å for the position of the discontinuity.

2228.2 – 4033. Osmer (1979) gives a very low-resolution plot of $\log f_\nu$ versus $\log \nu$. From this we estimate the position of the discontinuity to be at 3720 ± 40 Å.

From the foregoing summary it is reasonable to conclude that the position of the discontinuity lies in the vicinity of 3700 Å. We identify this discontinuity with the helium discontinuity at λ3680 (the ionization limit from the 2^1P^0 state of helium). While absorption lines from the $2^1P^0 - n^1D$ series have been observed in stellar spectra up to λ3737 (Thackeray, 1954) and λ3744 (Klemola, 1961; Drilling, 1973, 1978), to the best of our knowledge, it is the first time that the helium λ3680 discontinuity has been identified in an astronomical spectra. Our arguments in support of this identification are as follows. A good many absorption lines arising rom the 2^1P^0 level are observed in 0420 – 388. The Balmer discontinuity lies quite near the observed value, but as discussed earlier, in the available data, there is no clear evidence for the presence of hydrogen. However, should future investigations show the presence of the Balmer series, then admittedly, our conclusion will require reconsideration.

It would have been of interest to compare the colours of the seven quasars in Table I. But, unfortunately, data are available for only one of them, namely 0420 – 388, for which the values are: $B - V = 0.78$, $U - B = 0.90$ (Hewitt and Burbidge, 1987),

© Kluwer Academic Publishers • Provided by the NASA Astrophysics Data System

$J - H = 0.63 \pm 0.11$, $H - K = 0.48 \pm 0.16$ (Hyland and Allen, 1982). In analogy with what we found for 0237 – 233 (Varshni, 1988c) we expect that on the $(U - B)$, $(B - V)$ and $(J - H)$, $(H - K)$ plots the seven quasars will lie in close proximity.

Recently a quasar, 0420 – 388B (R.A. $4^h20^m36^s.6$, Decl. $-38°50'10''$, $V \simeq 20.8$) has been discovered (Cristiani and Shaver, 1988) which lies only 2.1 arc min away from 0420 – 388. It is possible that the two form a wide binary system.

5. Predictions

We make the following predictions:

(1) Under high-dispersion and high-resolution, absorption lines due to HeI will be observed in the other six quasars also.

(2) Narrow-band spectrophotometry would show that the discontinuity in the continuum in all the seven quasars (Table I) is close to $\lambda 3680$.

References

Aller, L. H.: 1963, *Astrophysics: The Atmospheres of the Sun and Stars*, The Ronald Press, New York.

Atwood, B., Baldwin, J. A., and Carswell, R. F.: 1985, *Astrophys. J.* **292**, 58.

Chalonge, D. and Divan, L.: 1952, *Ann Astrophys.* **15**, 201.

Cristiani, S. and Shaver, P.: 1988, in F. Bertola, J. W. Sulentic, and B. F. Madore (eds.), *New Ideas in Astronomy*, Cambridge University Press, Cambridge, p. 155.

Drilling, J. S.: 1973, *Astrophys. J.* **179**, L31.

Drilling, J. S.: 1978, *Astrophys. J.* **223**, L29.

Foltz, C. B., Chaffee, Jr., F. H., Hewett, P. C., MacAlpine, G. M., Turnshek, D. A., Weymann, R. J., and Anderson, S. F.: 1987, *Astron. J.* **94**, 1423.

Hewitt, A. and Burbidge, G. R.: 1987, *Astrophys. J. Suppl.* **63**, 1.

Hyland, A. R. and Allen, D. A.: 1982, *Monthly Notices Roy. Astron. Soc.* **199**, 943.

Kaufmann, J. P. and Theil, U.: 1980, *Astron. Astrophys. Suppl.* **41**, 271.

Klemola, A. R.: 1961, *Astrophys. J.* **134**, 130.

Kunth, D., Sargent, W. L. W., and Kowal, C.: 1981, *Astron. Astrophys. Suppl.* **44**, 229.

Moore, C. E. and Merrill, P. W.: 1968, *Partial Grotrian Diagrams of Astrophysical Interest*, NSRDS-NBS 23, U.S. Government Printing Office, Washington, D.C.

Osmer, P. S.: 1979, *Astrophys. J.* **227**, 18.

Osmer, P. S.: 1980, *Astrophys. J. Suppl.* **42**, 523.

Osmer, P. S. and Smith, M. G.: 1977, *Astrophys. J.* **215**, L47.

Shaver, P. A., Boksenberg, A., and Robertson, J. G.: 1982, *Astrophys. J.* **261**, L7.

Smith, M. G., Carswell, R. F., Whelan, J. A. J., Wilkes, B. J., Boksenberg, Clowes, R. G., Savage, A., Cannon, R. D., and Wall, J. V.: 1981, *Monthly Notices Roy. Astron. Soc.* **195**, 437.

Thackeray, A. D.: 1954, *Monthly Notices Roy. Astron. Soc.* **114**, 93.

Varshni, Y. P.: 1973, *Bull. Am. Phys. Soc.* **18**, 1384.

Varshni, Y. P.: 1974, *Bull. Am. Astron. Soc.* **6**, 213, 308.

Varshni, Y. P.: 1975, *Astrophys. Space Sci.* **37**, L1.

Varshni, Y. P.: 1976, *Astrophys. Space Sci.* **43**, 3.

Varshni, Y. P.: 1977a, *Astrophys. Space Sci.* **46**, 443.

Varshni, Y. P.: 1977b, *J. Roy. Astron. Soc. Canada* **71**, 403.

Varshni, Y. P.: 1978, in S. Fujita (ed.), *The Ta-You Wu Festschrift: Science of Matter*, Gordon and Breach, New York, p. 285.

Varshni, Y. P.: 1979, *Phys. Canada* **35**, 11.

Varshni, Y. P.: 1981, *Astrophys. Space Sci.* **74**, 3.

Varshni, Y. P.: 1982, *Spec. Sci. Tech.* **5**, 521.

© Kluwer Academic Publishers • Provided by the NASA Astrophysics Data System

Varshni, Y. P.: 1983, *Sov. Astron. Lett.* **9**, 368.
Varshni, Y. P.: 1985, *Astrophys. Space Sci.* **117**, 337.
Varshni, Y. P.: 1988a, *Bull. Am. Astron. Soc.* **20**, 733.
Varshni, Y. P.: 1988b, *Bull. Am. Phys. Soc.* **33**, 1184.
Varshni, Y. P.: 1988c, *Astrophys. Space Sci.* **149**, 197.
Varshni, Y. P. and Lam, C. S.: 1976, *Astrophys. Space Sci.* **45**, 87.
Varshni, Y. P. and Nasser, R. M.: 1986, *Astrophys. Space Sci.* **125**, 341.
Vaucher, B. G., Kreidl, T. J., Thomas, N. G., and Hoag, A. A.: 1982, *Astrophys. J.* **261**, 18.
Walker, G.: 1987, *Astronomical Observations*, Cambridge University Press, Cambridge.
Weedman, D. W.: 1985, *Astrophys. J. Suppl.* **57**, 523.
Wilkes, B. J.: 1986, *Monthly Notices Roy. Astron. Soc.* **218**, 331.
Wilkes, B. J., Wright, A. E., Jauncey, D. L., and Peterson, B. A.: 1983, *Proc. Astron. Soc. Australia* **5**, 2.
Wolstencroft, R. D., Ku, W. H. M., Arp, H. C., and Scarrott, S. M.: 1983, *Monthly Notices Roy. Astron. Soc.* **205**, 67.
Wright, A. E., Peterson, B. A., and Jauncey, D. L.: 1979, *Monthly Notices Roy. Astron. Soc.* **188**, 711.
Wright, A. E., Peterson, B. A., Jauncey, D. L., and Condon, J. J.: 1978, *Astrophys. J.* **226**, L61.
Wright, A. E., Peterson, B. A., Jauncey, D. L., and Condon, J. J.: 1979, *Astrophys. J.* **229**, 73.

© Kluwer Academic Publishers • Provided by the NASA Astrophysics Data System